Available online at www.sciencedirect.com

SCIENCE DIRECT

Brain Research 1044 (2005) 164 – 175

BRAIN RESEARCH

www.elsevier.com/locate/brainres

Research report

Axonal and extracellular matrix responses to experimental chronic nerve entrapment

Rafael Augusto Dantas Prinz[a], Marcos Nakamura-Pereira[a], Bernardo De-Ary-Pires[a], Daniel Fernandes[a], Bárbara Daphne Souza Valle Fabião-Gomes[a], Ana Maria Blanco Martinez[b], Ricardo de Ary-Pires[a], Mário Ary Pires-Neto[a,*]

[a]*Departamento de Anatomia, Universidade Federal do Rio de Janeiro, CCS, Bloco F, Cidade Universitária, 21941-590, Rio de Janeiro, Brazil*
[b]*Departamento de Histologia e Embriologia, Universidade Federal do Rio de Janeiro, Brazil*

Accepted 23 February 2005
Available online 15 April 2005

Abstract

We have analyzed the ultrastructural and histopathological changes that occur during experimental chronic nerve entrapment, as well as the immunohistochemical expression of chondroitin sulfate proteoglycan (CSPG). Adult hamsters (n = 30) were anesthetized and received a cuff around the right sciatic nerve. Animals survived for varying times (5 to 15 weeks) being thereafter perfused transcardially with fixative solutions either for immunohistochemical or electron microscopic procedures. Experimental nerves were dissected based upon the site of compression (proximal, entrapment and distal). CSPG overexpression was detected in the compressed nerve segment and associated with an increase in perineurial and endoneurial cells. Ultrastructural changes and data from semithin sections were analyzed both in control and compressed nerves. We have observed endoneurial edema, perineurial and endoneurial thickening, and whorled cell-sparse pathological structures (Renaut bodies) in the compressed nerves. Morphometrical analyses of myelinated axons at the compression sites revealed: (a) a reduction both in axon sectional area (up to 30%) and in myelin sectional area (up to 80%); (b) an increase in number of small axons (up to 60%) comparatively to the control group. Distal segment of compressed nerves presented: (a) a reduction in axon sectional area (up to 60%) and in myelin sectional area (up to 90%); (b) a decrease in axon number (up to 40%) comparatively to the control data. In conclusion, we have shown that nerve entrapment is associated with a local intraneural increase in CSPG expression, segmental demyelination, perineurial and endoneurial fibrosis, and other histopathological findings.

Theme: Development and regeneration
Topic: Regeneration

Keywords: Peripheral nervous system; Nerve injury; Nerve regeneration; Neuropathy

1. Introduction

Entrapment neuropathy is a group of clinical disorders that are produced by existing anatomical arrangements that cause compression or constriction of a peripheral nerve, interfering with nerve function mostly through traction injury. Such syndromes occur at specific places where nerves are confined to narrow anatomical pathways and therefore are intensely susceptible to constraining pressures. In those neuropathies, the neural lesion is directly attributable to local causes comprising disturbances to nerve vascular supply [23], axonal transport mechanisms [10,52], degeneration of myelin sheaths [26,60], axonal damage [61], and/or connective tissue changes such as endoneurial edema [27,43,59]. Both ischemic and mechanical factors are involved in the development of compression neuropathy [33].

* Corresponding author. Fax: +55 21 25536321.
E-mail address: mapneto@rionet.com.br (M.A. Pires-Neto).
URL: http://www.neuroanatomia.org (M.A. Pires-Neto).

0006-8993/$ - see front matter © 2005 Elsevier B.V. All rights reserved.
doi:10.1016/j.brainres.2005.02.085

Proteoglycans exert recognizable influences on aging and plasticity of the nervous system [20,48]. Chondroitin sulfate proteoglycans (CSPGs) are important molecules in developmental events, such as axonal growth, pathfinding, and boundary formation. Interestingly, CSPGs are generally inhibitory to neurite outgrowth [54], albeit during development CSPGs provide cues for axonal guidance. Notwithstanding, following nervous system injury in aging and degenerative diseases (e.g., Alzheimer's disease), CSPGs block thorough regeneration and hinder axonal regrowth after neural lesions [12]. This fact can be undeniably supported by the finding that axonal regeneration is enhanced following treatment of the injured central nervous system (CNS) with enzymes that cleave CSPGs, such as chondroitinase ABC [5,20,25,28,39,53,64,65]. CSPGs are also overexpressed in various neurodegenerative [13,40] and demyelinating diseases [58]. Besides, CSPGs are regularly present in peripheral nerve sheaths and interstitial tissues [28,67]. In the present study, we investigate the ultrastructural, histopathological and immunohistochemical expression of CSPG in chronically compressed sciatic nerves endeavoring to clarify a few of the intricate processes associated with nerve entrapment syndromes. Peripheral nerve lesions induced by chronic compression were also qualitatively and quantitatively analyzed by light and electron microscopy in order to detect tissue changes evoked by entrapment.

2. Materials and methods

All procedures in the present investigation are in full agreement with the regulations of the Animal Care and Use Committee of the Federal University of Rio de Janeiro (Brazil) and conform to the standards for use of laboratory animals established by the National Institute of Health Guide for the Care and Use of Laboratory Animals (NIH Publications No. 80-23, revised 1996) and also by the European Communities Council Directive of 24 November 1986 (86/609/EEC).

2.1. Animals

Adult hamsters (*Mesocricetus auratus*, n = 30) were deeply anesthetized with a 25% pentobarbital solution and each animal received a surgically applied silicone cuff (length = 1.0 cm and luminal diameter = 1.0 mm) embracing the right sciatic nerve. The normal sciatic nerve of adult hamsters presents a diameter of approximately 1.0 mm. The left sciatic nerves were not operated and represented the control group. After surgery, animals were kept under veterinary care for variable survival intervals (5–15 weeks), after which they were sacrificed by ether inhalation. Thereafter, animals were immediately perfused transcardially with saline (0.9% NaCl) followed by fixative solution (4% paraformaldehyde in 0.1 M sodium phosphate buffer, pH 7.4). Sciatic nerves were meticulously dissected out and divided into segments based upon their distance from the site of nerve compression (proximal, entrapment and distal). Proximal nerve segment (length = 5 mm) was considered to be a nerve region that was separated from the entrapment segment by an intermediate zone of approximately 3 mm in length (Fig. 1). Entrapment nerve segment (length = 10 mm) was collected at the site of compression. Distal nerve segment (length = 5 mm) was obtained from a region separated from the entrapment segment by an intermediate zone of approximately 3 mm in length. For immunohistochemical study, nerves were immersed in graded (10–20%) sucrose solutions diluted in 2% paraformaldehyde in 0.1 M sodium phosphate buffer, pH 7.4 for cryoprotection.

2.2. Immunohistochemistry

Immunohistochemical labeling was performed using primary monoclonal antibody for CSPG (CS-56, Sigma Chemical, USA; dilution 1:200). The following secondary antibody was used: Cy3-conjugated goat anti-mouse IgG (Jackson ImmunoResearch Laboratories, USA, dilution 1:100). Antibodies were diluted in phosphate buffer saline (PBS) mixed with 0.05% triton-X-100 at pH 7.4.

After sucrose cryoprotection, nerves were embedded in a medium appropriate for frozen tissue specimens (Tissue-Tek, OCT compound, Sakura Finetek, USA). Cryosection was performed (Cryocut 1800, Reichert-Jung, Germany) at 7 μm along the sagittal, coronal and horizontal planes of different nerve segments. The resulting sections were collected on gelatin-chrome alum-coated slides that were left drying for a few hours at 37 °C. After 3 washes in PBS

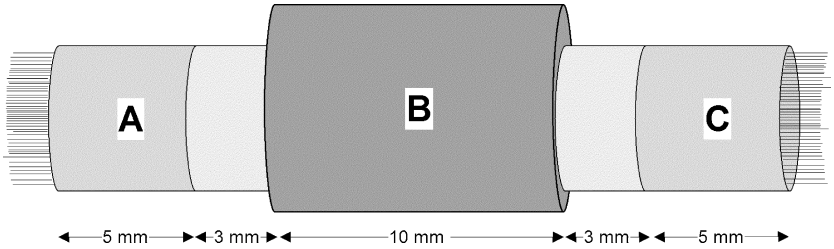

Fig. 1. Schematic drawing of the compressed sciatic nerve. A small silicone cuff was surgically applied embracing the right sciatic nerve. After variable survival intervals, the nerves were dissected and divided into segments based upon their distance from the site of compression. We represent the proximal (A), the entrapment (B), and the distal (C) nerve segments with chronic compression. Distances are shown in millimeters (mm).

mixed with 0.05% triton-X-100 for 5 min each, and 40 min in 10% normal goat serum (NGS, Sigma Chemical, USA), primary antibody was gently pipetted (50 μL/tissue section) over the slides that were subsequently maintained in a humidifier chamber overnight at 4 °C. After three further washes in PBS, secondary antibodies were applied to the sections for 1.5 h in the dark at room temperature. Tissue sections were rinsed in PBS and immersed for 1 min in a solution of 4′,6-diamidino-2-phenylindole (DAPI, Sigma Chemical, USA): one crystal in 10 mL of PBS, for nuclear counterstaining. N-propyl-gallate (Sigma Chemical, USA) was used as an anti-fading agent, and coverslips were applied to the sections. The sections were examined under a fluorescent microscope (Axioplan, Carl Zeiss, Brazil) equipped with rhodamine (Zeiss BP 546/FT 580/LP 590) and ultraviolet filters (Zeiss BP 365/FT 395/LP 397). Photographs were scanned (Hewlett-Packard 4C Scanner), contrasted and sized appropriately using a photo-editing software (Adobe Photo Shop 8.0).

2.3. Light and electron microscopy

After animal perfusion, nerve segments were excised and immersed in a glutaraldehyde solution (2% glutaraldehyde in 0.1 M cacodylate buffer, pH 7.4) for 2 h followed by 1% osmium tetroxide with 0.8% potassium ferricyanide and $CaCl_2$ in 0.1 M cacodylate buffer, pH 7.4 for 1 h. Nerve blocks were subsequently dehydrated in graded acetone solutions and embedded in PolyBed 812 resin. Semithin (500 nm) and ultrathin (60–70 nm) sections were stained with toluidine blue, uranyl acetate and lead citrate, respectively. Ultrathin sections were examined under a Zeiss EM-900 (Carl Zeiss, Oberkochen, Germany) electron microscope. Semithin sections of both control and compressed nerves were photographed with a light microscope (Axioscope, Zeiss) and then analyzed morphometrically (Image Pro Plus 4.5, Media Cybernetics, Carlsbad, CA, USA). Measurements were taken for linear dimensions (maximal and minimal axonal and myelin cross-sectional diameter and perimeter), cross-sectional areas (axonal and myelin sheath areas) and counting of axon number in the central and marginal regions of the nerve. All morphometric evaluations were repeated for at least three consecutive trials and average values were calculated thereafter. Morphometrical procedures were performed in agreement with well-known methodologies for systematic nerve quantification [51]. Central nerve regions were compared to marginal nerve regions in each experimental group. The central region of the sciatic nerve was defined as the inner circular zone corresponding to 50% of the nerve diameter, surrounded by an outer frame or marginal region corresponding to 25% of the nerve diameter on each extremity of the transverse section. Myelinated axons in both nerve regions were systematically counted with the use of a uniform sampled area (3600 μm^2 grid) and the data were respectively expressed as a percentage of axon number (mean ± Standard Error of the Mean—SEM). It was assumed that axon number in the central or marginal regions of the control nerves represented 100% of the normal axon population in each respective region. In addition, axon sectional area (AA = axon area), myelin sectional area (MA = myelin sheath area) and also the total fiber sectional area (TA = data including both the axon and myelin areas) were analyzed in each nerve segment. Moreover, the g ratio (axon diameter/total fiber diameter) was calculated for each nerve fragment analyzed. Statistical analysis of the data was performed with a computerized package (SPSS 12.0 for MS Windows, SPSS, USA). Data were shown to be homoscedastic (Bartlett's test) and to follow a Gaussian distribution (Kolmogorov–Smirnov's and Shapiro–Wilk's tests). Detailed comparisons among different groups consisted of bivariate analysis of variance (ANOVA) with Duncan's multiple range post hoc test ($P < 0.01$).

3. Results

After surgery, the main pathologic findings were already thoroughly established after a 5-week survival interval and most alterations followed a similar pattern of presentation in animals enduring longer compression (up to 15 weeks).

3.1. CSPG overexpression in experimental chronic nerve compression

Immunohistochemical assays revealed an overexpression of CSPG within the compressed sciatic nerve segment in comparison with the control group (Fig. 2). CSPG was observed to be concentrated in the perineurial and adjoining endoneurial layers in close proximity to the site of compression. Both perineurial and endoneurial CSPG labeling were more intensely detected on cross-sectional areas from entrapped nerves in comparison with similar areas obtained from control nerves. Often, high CSPG expression could be identified both in the marginal and along variable portions of the central nerve regions, forming a densely arranged proteoglycan mass, and leaving only a relatively narrow core of unlabeled cross-sectional area of the nerve. This CSPG altered pattern could seen as early as after 5 weeks of survival (Fig. 2C) and is remarkably accentuated after 15 weeks of nerve compression (Fig. 2A). Control nerves exhibit low intensity of CSPG labeling (Fig. 2E). Furthermore, DAPI counterstaining revealed a severely disorganized cellular arrangement located in the marginal and juxtaposed central nerve regions, exhibiting a circumferential pattern in entrapped nerves (Figs. 2B and D) instead of the laminar arrangement observed in the control group (Fig. 2F).

3.2. Tissue changes promoted by entrapment in nerve morphology

Ultrastructural nerve morphology exhibited endoneurial edema, in association with thickening of both endoneurium

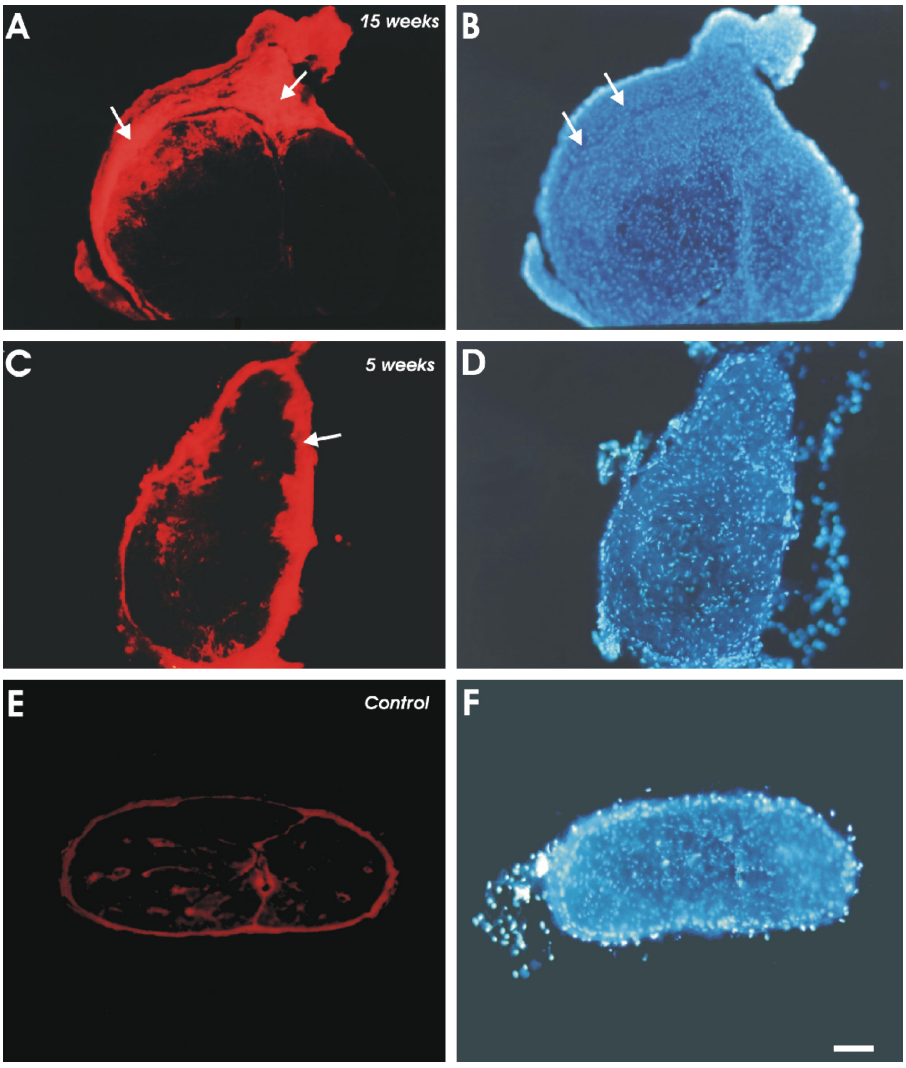

Fig. 2. Immunohistochemical labeling for CSPG in transverse sections of the sciatic nerve. (A) CSPG overexpression (white arrows) after chronic nerve entrapment (about 15 weeks); (B) same field as (A) with DAPI counterstaining, exhibiting an altered pattern of cellular layers (white arrows). (C) CSPG overexpression after 5 weeks of nerve entrapment; (D) same field as (C) with DAPI counterstaining, exhibiting a moderate disarrangement of the cellular layers. (E) CSPG basal expression in control sciatic nerve; (F) same field as (E) with DAPI counterstaining, presenting the normal cellular pattern of the sciatic nerve. Calibration Bar = 150 μm, same for all figures.

and perineurium, implying a distinct displacement of nerve fibers. The *vasa nervorum* pattern was also altered in compressed sciatic nerves comparatively to the control group. Intense myelin sheath degeneration was also observed at the entrapment site and mainly in the distal segment along with a concomitant influx of fibroblasts and Schwann cells to the lesioned regions (Fig. 3).

We also observed loosely-textured and whorled cell-sparse structures, ranging from 15 to 145 μm in diameter, found in the subperineurial space of the compressed sciatic nerve (Fig. 4). These structures represent Renaut bodies that represent nerve cell-sparse structures with a predilection for sites of nerve compression and mechanical stress [2]. In these areas, we often observed isolated nerve fibers surrounded by collagen fibers. In transverse semithin sections of the entrapped nerve, Renaut bodies display a roughly spherical outline with a whorled cell-sparse appearance and always lie in a subperineurial layer (Fig. 5). The adjacent nerve fibers sometimes appear to be displaced away from the Renaut body, although such nerve fibers generally show no pathologic changes. In longitudinal sections, Renaut bodies are seen to extend for large distances, frequently ending in an abrupt manner as a rounded extremity. In electron micrographs, the Renaut body is composed of loosely arranged, randomly oriented collagen fibers and large amounts of fine fibrillar material. Most of the cells within a Renaut body are identified by electron microscopy as fibroblasts. This finding is based upon the nature of their cytoplasmic processes and organelles, and the absence of basement membrane. An occasional cell may be observed partially enclosed by a basement membrane, suggesting an alternate identity, possibly representing either a pericyte or a perineurial cell.

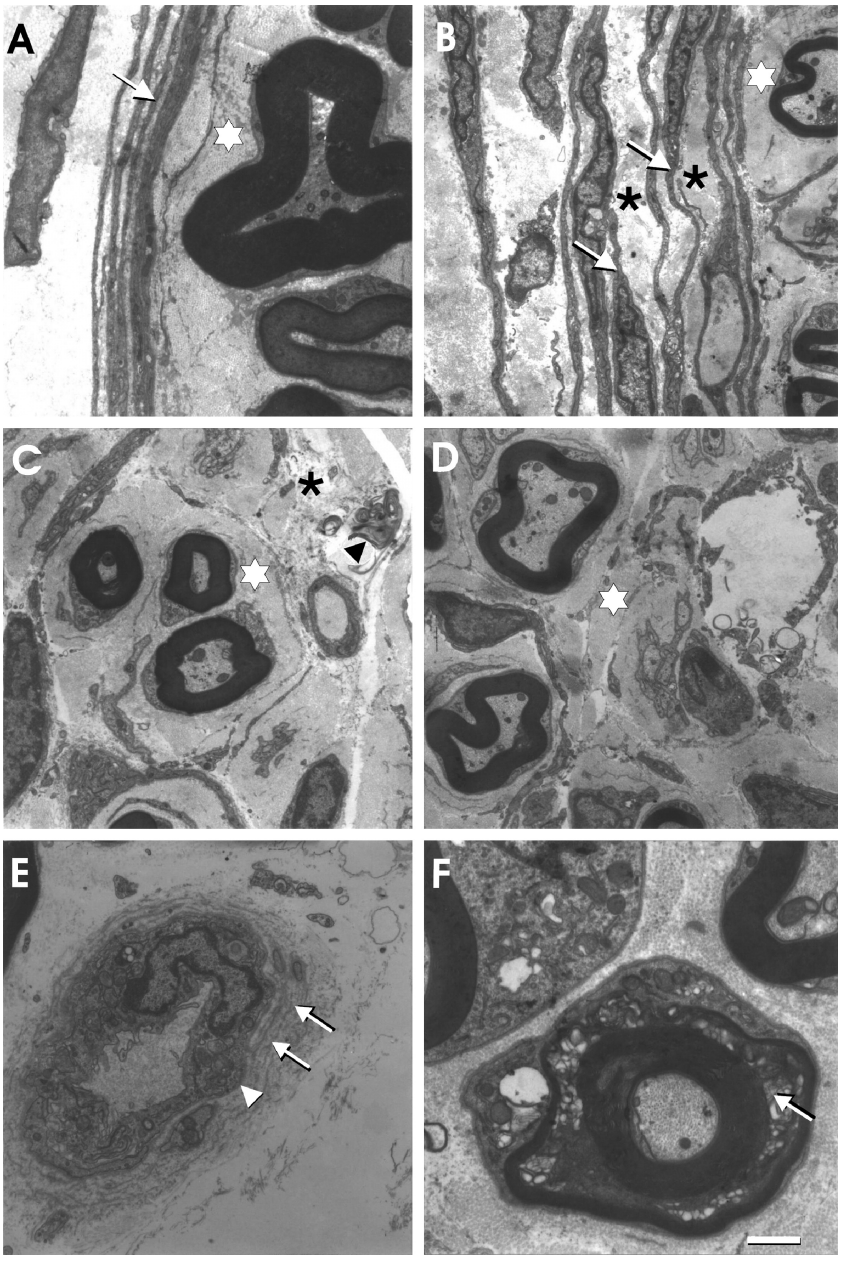

Fig. 3. Transmission electron microscopy of the sciatic nerve. (A) Normal sciatic nerve exhibiting well preserved perineurium (arrow), endoneurium (white asterisk), and myelinated nerve fibers. Figures from B to F display entrapped sciatic nerves after 5 weeks of survival. (B) Thickened perineurium presenting alternating layers of collagen fibrils (black stars) and perineurial cells and processes (arrows). At the right side of the picture, we can observe myelinated nerve fibers and endoneurium (white asterisk). (C and D) Transverse sections of the nerve displaying myelinated nerve fibers among areas of endoneurium thickening (white asterisks) and edema (black star in Figure C). Also, in figure C, we can observe myelin sheath debris (black arrowhead) in the endoneurium. (E) Endoneurium vessel presenting a thick wall formed by enlarged endothelial cell wrapped by a basal lamina (white arrowhead) and perineurial-like sheaths (white arrows). (F) Cross-section of a myelinated nerve fiber displaying extensive vacuolization of the myelin sheath (white arrow). Calibration bars are in A = 1.5 μm; B = 2.8 μm; C and D = 2.0 μm; E = 1.5 μm; F = 0.8 μm.

3.3. Morphometric analysis of the sciatic nerves: investigation upon the morphological effects of chronic entrapment after 5 weeks of survival

The number of myelinated axons in each nerve segment – control (CTR), proximal (PRX), entrapment (ENT) and distal (DIS) – was analyzed according to axonal position either in the central (CEN) or marginal (MAR) region of the nerve. Data are reported as a percentage of the respective control region (Fig. 6). Interestingly, the results observed at the entrapment site displayed a remarkable increase in the number of small axons either in the central (26.36 ± 12.48%) or marginal (53.54 ± 8.92%) nerve region after 5 weeks of survival in comparison with the axonal number in the control group. In addition, the distal segment of the compressed nerve presented a distinct decrease in axon

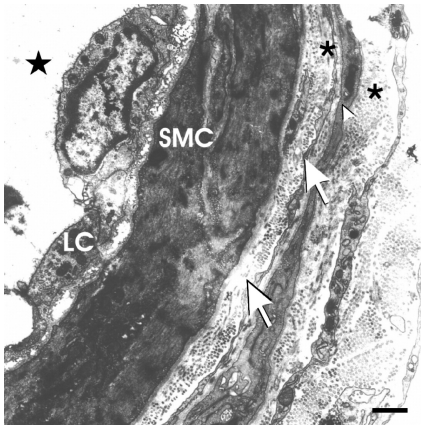

Fig. 4. Transverse section through a Renaut body showing a thick wall composed by alternating layers of collagen fibrils (small black stars) fibroblast/perineurial cells and processes (white arrows and white arrowhead), and a probable smooth muscle cell cytoplasm (SMC) and elongating lining cells (LC). Entrapped sciatic nerve after 5 weeks of survival. The left upper corner of the picture represents the lumen of the Renaut body filled with amorphous material (big black star). Scale bar = 0.7 μm.

number in both the central (34.29 ± 4.44%) and marginal (24.04 ± 3.68%) entrapped nerve regions comparatively to control nerves.

The sectional areas of myelinated nerve fibers in each nerve segment – control (CTR), proximal (PRX), entrapment (ENT) and distal (DIS) – were also analyzed according to axonal position either in the central (CEN) or marginal (MAR) region of the nerve (Fig. 7). Furthermore, we compared each morphometric sectional area

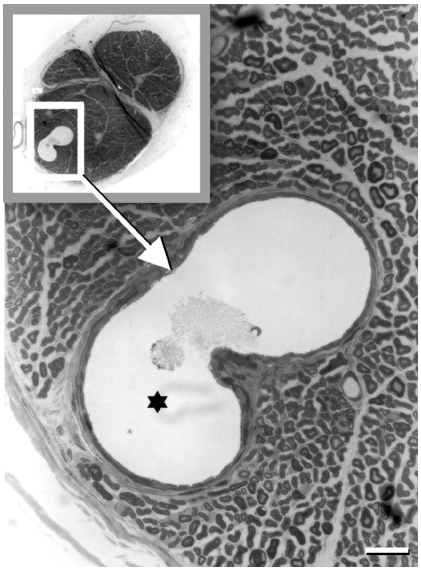

Fig. 5. Semithin section through an entrapped nerve segment (after 5 weeks of survival) displaying a spherical pathological structure (Renaut body). Inset shows the relative position of a Renaut body in a transverse nerve section. White arrow points at a magnified view of the same region, evidencing the displacement of myelin fibers by the Renaut body. The luminal space of the Renaut body is marked by a black asterisk. Calibration bar = 20 μm.

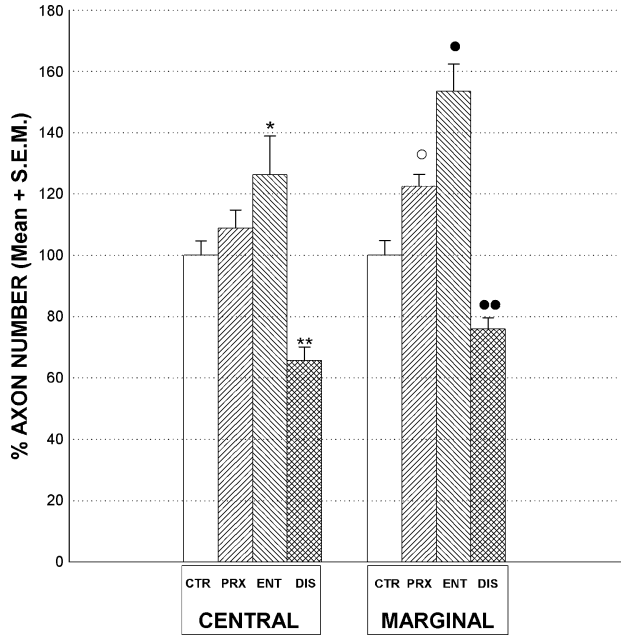

Fig. 6. The number of myelinated axons observed in semithin sections of each nerve segment – control (CTR), proximal (PRX), entrapment (ENT) and distal (DIS) – was analyzed according to axonal position either in the central or marginal sciatic nerve regions. The number of axons in the respective region of the CTR was assumed to be 100%. Data are reported as means ± SEM (standard error of the mean). Entrapped sciatic nerves after 5 weeks of survival. All symbols placed on top of bars represent statistically different groups ($P < 0.01$) compared with respective control nerve region (Duncan multiple range test).

analyzed with other areas of all experimental groups (Fig. 8), as well as the axon/fiber ratio (g ratio) in each nerve segment (Fig. 9). The mechanical compression determined an increase in number of myelinated fibers with small sectional area (<3.5 μm^2) both in CEN and in MAR of PRX and ENT nerve segments. In the entrapped nerve region, clusters of small regenerating axons could be distinctively identified and were surrounded by other isolated and variably myelinated axons (Fig. 10).

4. Discussion

The present study has investigated the effects of experimental chronic nerve compression on the morphology of entrapped sciatic nerves of adult hamsters. The entrapment procedure used in this investigation produces the formation of recognizable neuropathological signs [7,34,38] at a faster rate than previously described for the compressed sciatic nerve of the rat [45]. A possible explanation for this discrepancy may be related either to intrinsic differences between the species used (hamsters instead of Sprague–Dawley rats) and/or to the methodology employed. We have used a silicone tube (length = 1.0 cm; luminal diameter = 1.0 mm) in order to compress the sciatic nerve (diameter = 1.0 mm) of adult hamsters. O'Brien et al's experiment used silastic tubes (length = 1.0 cm) with luminal diameter

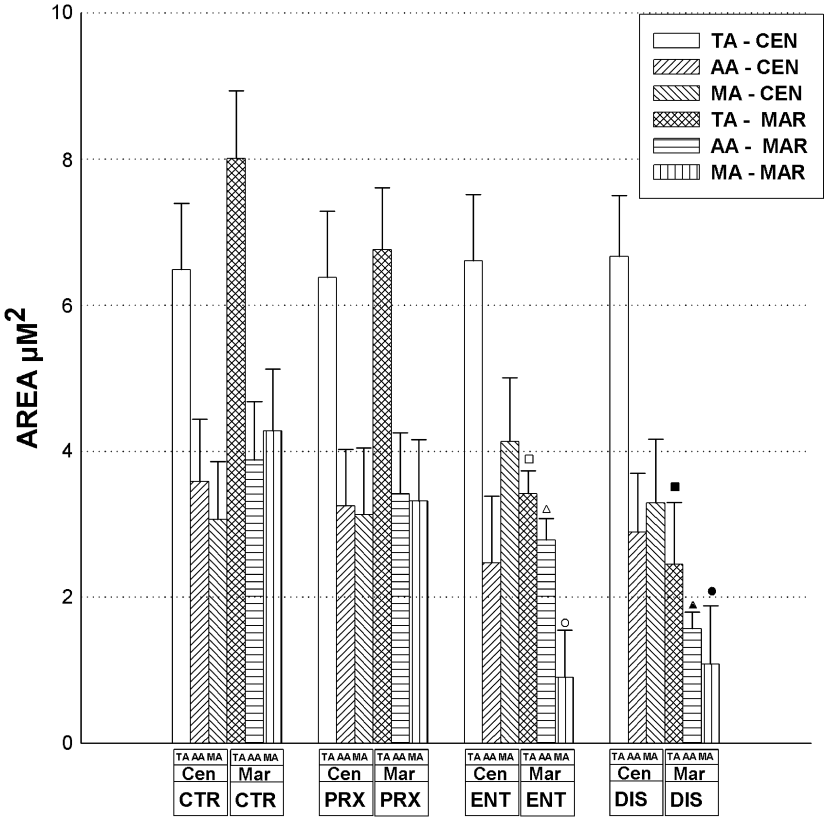

Fig. 7. The sectional areas of myelinated nerve fibers in each nerve segment – control (CTR), proximal (PRX), entrapment (ENT) and distal (DIS) – were analyzed according to axonal position either in the central (CEN) or marginal (MAR) region of the sciatic nerve. Axon sectional area (AA = axon area); myelin sectional area (MA = myelin area); and total fiber sectional area (TA = total area of the fiber, including both the axon and the myelin areas) were analyzed in each nerve segment. Entrapped sciatic nerves after 5 weeks of survival. All symbols placed on top of bars represent statistically different groups ($P < 0.01$) compared with respective control nerve region (Duncan multiple range test).

varying from 0.6 to 1.5 mm in order to compress the sciatic nerve (diameter = 1.3 mm) of adult rats. They observed Wallerian degeneration in experimental groups with tubes varying from 0.6 to 0.9 mm after 1 month of compression, displaying an intense reduction (50 to 75%) in nerve diameter. Interestingly, the experimental group with tubes of 1.1 mm presented perineurial fibrosis and reduction of myelinated fibers at the nerve peripheral zone due to chronic nerve compression after 2 months; the same results were obtained after 4 months with tubes of 1.5 mm in luminal diameter [45].

Mosconi and Kruger studied rat sciatic nerves previously submitted to chronic constriction with polyethylene cuffs of 0.028–0.030 in. inner diameter with the aim of inducing a standardized nerve injury. In such a model, they examined the temporal sequence of axonal degeneration and regeneration over a 6-week postoperative period [41]. In that chronic constriction injury (CCI) model, they compared the fiber-size spectrum between control and distal sciatic nerve sections and found that the number of small myelinated axons (<7 μm^2 area) was significantly elevated at 10 days postoperatively and remained higher than control values through 42 days. In addition, they found the number of large myelinated axons in the distal nerve sections to be reduced even at day 3, with maximum decrement at 7 days postoperatively, and remaining depressed through 42 days [41].

Most researchers agree that the primary morphological effect of CCI on the nerve distally to the ligatures is a profound disruption in the populations of large- to medium-caliber myelinated axons [3,8,9,18,22,41,42,44].

Chronic compressive neuropathies were analyzed by various researchers on both human nerve tissues and experimental models [7,11,29,33–37]. Electrodiagnostic studies revealed that in the majority of patients with compressive neuropathies, the symptoms related directly to problems involving the connective tissue of the nerve rather than pathologies of the nerve fiber [33].

Along the entrapped nerve segment, it was also possible to identify Renaut bodies that contained a loosely textured amorphous and fibrillar material [16,55,63]. Originally described in 1881 by Joseph Louis Renaut, the structures which carry his name, the Renaut bodies [50], were characterized as large (20 to 500 µm in transverse diameter), well-demarcated elliptical structures with an onion-skin arrangement of loosely textured, filamentous hyaline strands intermixed with sparse numbers of dark spindle-shaped nuclei [16,46].

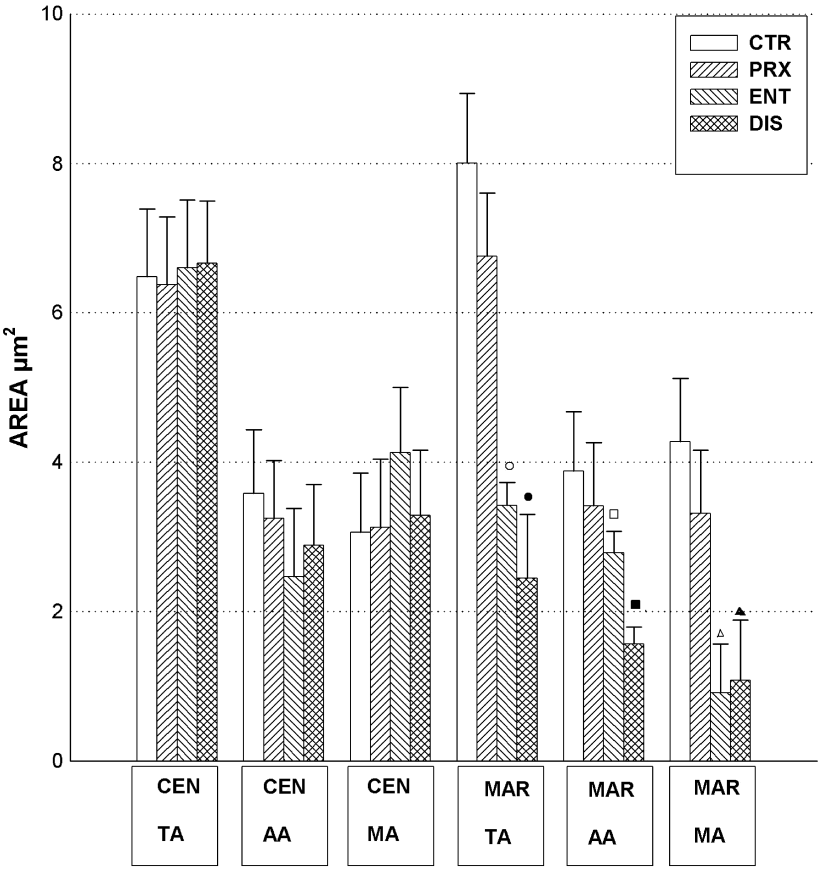

Fig. 8. Comparative analysis of each sectional area morphometrically analyzed (TA = total fiber area; AA = axonal area; and MA = myelin area) both in central (CEN) and in marginal (MAR) sciatic nerve regions of the various groups: control, proximal, entrapment, and distal nerve segments. Entrapped sciatic nerves after 5 weeks of survival. All symbols placed on top of bars represent statistically different groups ($P < 0.01$) compared with respective control nerve region (Duncan multiple range test).

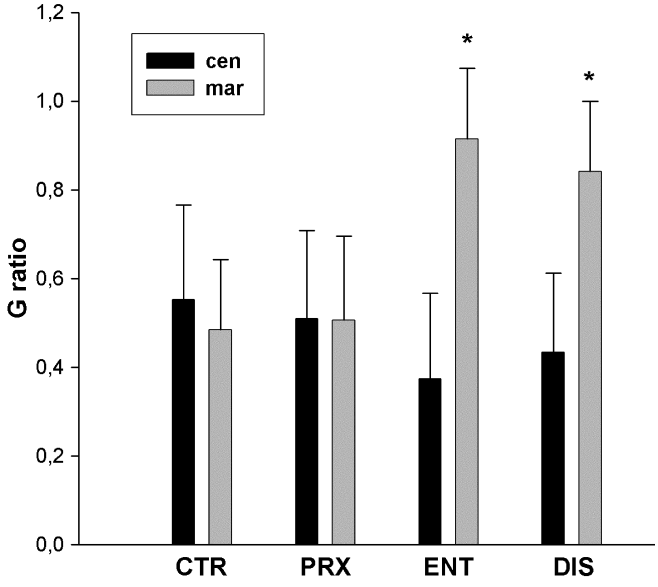

Fig. 9. The *g* ratio (axon diameter/total fiber diameter) for both central (CEN) and marginal (MAR) regions in control (CTR), proximal (PRX), entrapment (ENT) and distal (DIS) sciatic nerve regions analyzed. The *g* ratio displayed a distinct compromise of MAR observed in both ENT (0.92 ± 0.16) and DIS (0.84 ± 0.15) nerve segments. Entrapped sciatic nerves after 5 weeks of survival. All symbols placed on top of bars represent statistically different groups ($P < 0.01$) compared with respective control nerve region (Duncan multiple range test).

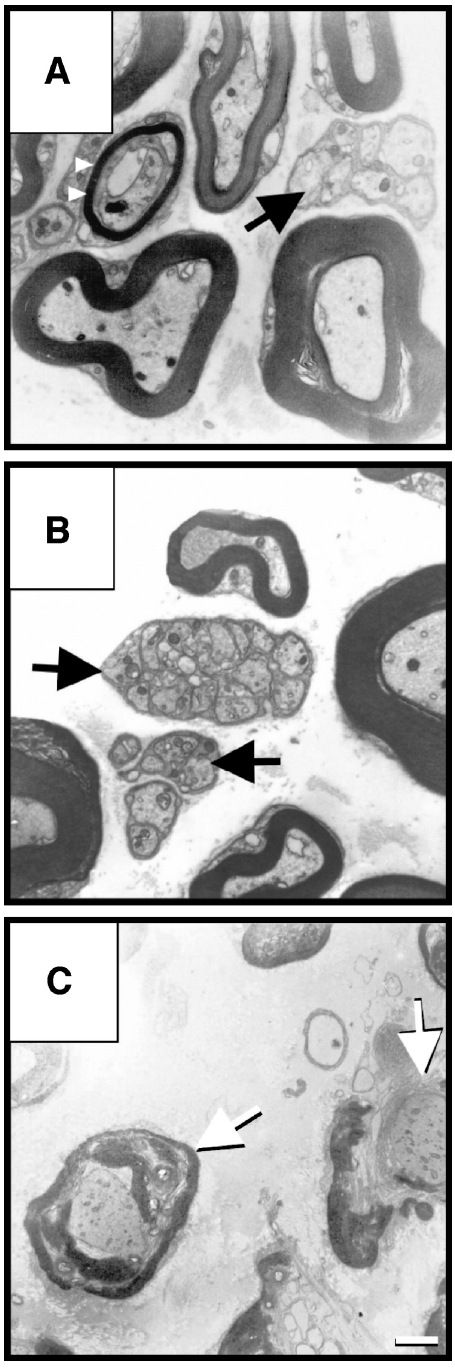

Fig. 10. Electron micrographs of the proximal segment of the compressed sciatic nerve showing clusters of regenerating axons (A and B—black arrows) and remyelinating fibers (white arrowheads). In C, partially demyelinated axons (white arrows) are observed. Entrapped sciatic nerves after 5 weeks of survival. Scale bar for A, B and C = 1.0 μm.

Renaut bodies exhibit mostly fibroblasts of perineurial and/or endoneurial origin with the extracellular matrix comprised of collagen fibrils, basal lamina material, and oxytalan filaments [55]. Renaut bodies seem to be derived mainly either from primary connective tissue elements of the endoneurium or from the degeneration of formed endoneurial structures such as capillaries. The latter possibility emerged from the study of human nerves showing close association between thickened endoneurial capillaries and Renaut bodies [2]. We have detected similar changes in the sciatic nerve of hamsters. Histological characteristics that differentiate Renaut bodies from malignant neurotropic infiltration are: (a) a cell-sparse mass, (b) absence of nuclear atypia, (c) a less extensive inflammatory infiltrate, and (d) well-defined borders [55]. We have observed in our experimental model, the basic morphological stages found in Renaut body formation [46]. These stages encompass: (a) endoneurial spaces appearance in the compressed nerve site, delimited by concentric layers of fibroblasts as an onion-like structure; (b) Gradual fusion of endoneurial cell-sparse spaces along with a concomitant formation of a fibrillary and amorphous material, rich in collagen fibrils, at the interior of the Renaut body. We have identified an increase in number of collagen fibrils, as well as in the total number of fibroblasts and Schwann cells in the endoneurial space, besides the thickening of the *vasa nervorum* (affecting the intima and media layer of the endoneurial vessels). In addition, we could also observe a segmental demyelination in both ENT and DIS segments, with a remarkable reduction in myelin sectional area of axons in those nerve regions.

The present model of experimental chronic nerve entrapment has been shown to promote a significant increase in axons of small diameter (less than 3 μm) at the site of compression. This finding may be largely attributable to axonal sprouting in response to nerve compression. This biological phenomenon was distinctly evident in the marginal region, where it could be statistically verified both in the proximal and in the entrapment nerve segments. Furthermore, we have found an important axonal degeneration occurring at the distal segment both in the central and in the marginal regions that may be considered as a plausible direct consequence of mechanical stress upon the sciatic nerve.

In the distal nerve segment, we have noticed endoneurial thickening with a prominent decrease in number of myelinated axons, as well as a decrease in myelin sectional area. Moreover, we have also verified a reduction both of MA and of AA parameters either in CEN or in MAR nerve regions. In contrast with ENT segment, where we have detected an increase in the number of myelinated axons of small diameter, DIS segment presented an important decrease in the number of myelinated axons affecting both CEN and MAR nerve regions.

The immunohistochemical analysis has revealed the overexpression of CSPG at the nerve entrapment segment, particularly in the MAR nerve region, and affecting both endoneurial and perineurial zones. We collected experimental evidences that the expression of CSPG in our model is proportionally increased with longer duration of nerve compression. The nuclear counterstaining with DAPI revealed a conspicuous increase in cell number at the entrapped nerve sites, in which we identified overexpression of CSPG, both in perineurial and in endoneurial

spaces. Previous findings support the idea that high concentrations of sulfated proteoglycans may regulate axonal growth during neural development and regeneration [1,4,6,48,57]. Although most studies implicate sulfated proteoglycans in the poor regenerative capacity of the central nervous system [17,19,21,30,40,54], inhibitory proteoglycans also may play an important role in the successful regeneration and guidance of axons within peripheral nerve [47,49,62,66,67]. An interesting and corroborating finding is provided by the enzymatic digestion (with chondroitinase ABC) of CSPG expressed at sites of CNS injury [5]. The consequent decrease in CSPG promotes significant axonal regrowth in a few experimental models [39,65]. Our electron microscopic results have revealed an increase in fibroblasts and Schwann cells mainly at the entrapped nerve sites, associated with clusters of sprouting axons, probably committed to regenerative processes. Based upon the aforementioned evidences and considering many of the roles attributed to CSPG in adult animals by several researchers, it is possible to suppose that CSPG may play a relevant pathological role involved at least with two important events observed in compressive neuropathy: (a) as a nonpermissive agent that could hamper regrowing nerve fibers and myelin formation; (b) as a space-occupying element that could produce an anfractuous path, highly unfavorable for recomposing normal nerve histology.

Sciatic nerve morphometric analysis in the central nerve region (CEN) has unveiled that: (a) TA (total fiber area) was similar between the control group and all three experimental nerve segments analyzed (PRX, ENT, and DIS), indicating that the central region of the nerve was roughly unaffected by this experimental chronic nerve entrapment model; (b) AA (axonal area) in all experimental groups was also statistically similar to the control central nerve region; (c) MA (myelin area) in all experimental groups in the central nerve region, was also comparable to the myelin area observed in the control sciatic nerve.

On the other hand, sciatic nerve morphometric analysis in the marginal nerve region (MAR) clarified the following points: (a) TA was dramatically affected both in ENT and DIS nerve regions, with a remarkable decrease in total sectional area of their nerve fibers; (b) AA exhibited a significant decrease in ENT and DIS, but was unaffected in the PRX nerve segment; (c) MA was drastically reduced both in ENT and DIS segments, but was also unaffected in PRX nerve segment.

The g ratio (axon diameter/total fiber diameter) for both CEN and MAR has displayed a distinct alteration in MAR observed in both ENT (0.92 ± 0.16) and DIS (0.84 ± 0.15) nerve segments (Fig. 9). The g ratio is closely related to nerve fiber morphofunctional integrity [24,56], and stresses the fact that, in our results, a major chronic compression was exerted on the marginal region of ENT and DIS segments, although the central region of those segments presented a compensatory increase in axon number, probably through axonal sprouting of regrowing nerve fibers.

Acute and chronic compression of a nerve affects its blood supply, the blood–nerve barrier, and the endoneurial fluid composition. Relatively low pressure impairs intraneural venous flow, alters vascular permeability and hence the blood–nerve barrier producing endoneurial edema. These changes modify the biochemical milieu of the nerve fibers, and the increased intrafascicular pressure may further contribute to nerve fiber dysfunction. Even modest pressure applied to a nerve impairs axonal transport, which may be another important factor in producing dysfunction in nerve compression [10,31,32,52].

The major histological changes that occur in large myelinated fibers submitted to chronic compression are similar to those seen in acute nerve compression and reveal combinations of segmental demyelination and Wallerian degeneration. Similar abnormalities are seen in experimentally-induced recurrent nerve compression and in an animal model that mimics chronic angulation and stretch [14,15].

In summary, we have provided morphological evidences of some major effects determined by experimental chronic entrapment of the sciatic nerve in adult hamsters. Certainly, further functional studies are necessary to clarify many of the neurobiological events related to peripheral nerve entrapment syndromes and their potential treatments.

Acknowledgments

This work was supported by grants from FAPERJ, CNPq, and CAPES. We are grateful to Adiel Nascimento, Antonia Lima Carvalho, Elizabeth Cunha Pena de Moraes and Jorge Luís da Silva for their excellent technical assistance.

References

[1] Ary-Pires R., Linden R., Laminin modulates neuritogenesis of developing rat retinal ganglion cells through a protein kinase C-dependent pathway, J. Neurosci. Res. 60 (2000) 291–301.
[2] Asbury A.K., Renaut bodies. A forgotten endoneurial structure, J. Neuropathol. Exp. Neurol. 32 (1973) 334–343.
[3] Basbaum A.I., Gautron M., Jazat F., Mayes M., Guilbaud G., The spectrum of fiber loss in a model of neuropathic pain in the rat: an electron microscopic study, Pain 47 (1991) 359–367.
[4] Bovolenta P., Fernaud-Espinosa I., Nervous system proteoglycans as modulators of neurite outgrowth, Prog. Neurobiol. 61 (2000) 113–132.
[5] Bradbury E.J., Moon L.D., Popat R.J., King V.R., Bennett G.S., Patel P.N., Fawcett J.W., McMahon S.B., Chondroitinase ABC promotes functional recovery after spinal cord injury, Nature 416 (2002) 636–640.
[6] Brittis P.A., Meiri K., Dent E., Silver J., The earliest patterns of neuronal differentiation and migration in the mammalian central nervous system, Exp. Neurol. 134 (1995) 1–12.
[7] Campbell W.W., Diagnosis and management of common compression and entrapment neuropathies, Neurol. Clin. 15 (1997) 549–567.

[8] Carlton S.M., Dougherty P.M., Pover C.M., Coggeshall R.E., Neuroma formation and numbers of axons in a rat model of experimental peripheral neuropathy, Neurosci. Lett. 131 (1991) 88–92.
[9] Coggeshall R.E., Dougherty P.M., Pover C.M., Carlton S.M., Is large myelinated fiber loss associated with hyperalgesia in a model of experimental peripheral neuropathy in the rat? Pain 52 (1993) 233–242.
[10] Dahlin L.B., Rydevik B., McLean W.G., Changes in fast axonal transport during experimental nerve compression at low pressures, Exp. Neurol. 84 (1984) 29–36.
[11] Da-Silva C.F., Langone F., Addition of nerve growth factor to the interior of a tubular prosthesis increases sensory neuron regeneration in vivo, Braz. J. Med. Biol. Res. 22 (1989) 691–694.
[12] DeWitt D.A., Silver J., Regenerative failure: a potential mechanism for neuritic dystrophy in Alzheimer's disease, Exp. Neurol. 142 (1996) 103–110.
[13] DeWitt D.A., Richey P.L., Praprotnik D., Silver J., Perry G., Chondroitin sulfate proteoglycans are a common component of neuronal inclusions and astrocytic reaction in neurodegenerative diseases, Brain Res. 656 (1994) 205–209.
[14] Duncan I.D., The neuropathy resulting from muscle–nerve translocation, Neuropathol. Appl. Neurobiol. 9 (1983) 195–206.
[15] Dyck P.J., Experimental hypertrophic neuropathy, Arch. Neurol. 21 (1969) 73–95.
[16] Elcock L.E., Stuart B.P., Hoss H.E., Crabb K., Millard D.M., Bopp B., Mueller R.E., Hastings T.F., Lake S.G., Renaut bodies in the sciatic nerve of beagle dogs, Exp. Toxicol. Pathol. 53 (2001) 19–24.
[17] Fitch M.T., Silver J., Glial cell extracellular matrix: boundaries for axon growth in development and regeneration, Cell Tissue Res. 290 (1997) 379–384.
[18] Gautron M., Jazat F., Ratinahirana H., Hauw J.J., Guilbaud G., Alterations in myelinated fibers in the sciatic nerve of rats after constriction: possible relationships between the presence of abnormal small myelinated fibres and pain behaviour, Neurosci. Lett. 111 (1990) 28–33.
[19] Gonzalez M.L., Silver J., Axon–glia interactions regulate ECM patterning in the postnatal rat olfactory bulb, J. Neurosci. 14 (1994) 6121–6131.
[20] Grimpe B., Silver J., The extracellular matrix in axon regeneration, Prog. Brain Res. 137 (2002) 333–349.
[21] Grimpe B., Dong S., Doller C., Temple K., Malouf A.T., Silver J., The critical role of basement membrane-independent laminin gamma 1 chain during axon regeneration in the CNS, J. Neurosci. 22 (2002) 3144–3160.
[22] Guilbaud G., Gautron M., Jazat F., Ratinahirana H., Hassig R., Hauw J.J., Time course of degeneration and regeneration of myelinated nerve fibres following chronic loose ligatures of the rat sciatic nerve: can nerve lesions be linked to the abnormal pain-related behaviours, Pain 53 (1993) 147–158.
[23] Harrison M.J.G., Pressure palsy of the ulnar nerve with prolonged conduction block, J. Neurol., Neurosurg. Psychiatry 39 (1976) 96–99.
[24] Hildebrand C., Bowe C.M., Remahl I.N., Myelination and myelin sheath remodelling in normal and pathological PNS nerve fibres, Prog. Neurobiol. 43 (1994) 85–141.
[25] Inman D.M., Steward O., Ascending sensory, but not other long-tract axons, regenerate into the connective tissue matrix that forms at the site of a spinal cord injury in mice, J. Comp. Neurol. 462 (2003) 431–449.
[26] Jefferson D., Eames R.A., Subclinical entrapment of the lateral femural cutaneous nerve, Muscle Nerve 2 (1979) 145–154.
[27] Kale B., Yuksel F., Celikoz B., Sirvanci S., Ergun O., Arbak S., Effect of various nerve decompression procedures on the functions of distal limbs in streptozotocin-induced diabetic rats: further optimism in diabetic neuropathy, Plast. Reconstr. Surg. 111 (2003) 2265–2272.
[28] Krekoski C.A., Neubauer D., Zuo J., Muir D., Axonal regeneration into acellular nerve grafts is enhanced by degradation of chondroitin sulfate proteoglycan, J. Neurosci. 21 (2001) 6206–6213.
[29] Langone F., Lora S., Veronese F.M., Caliceti P., Parnigotto P.P., Valenti F., Palma G., Peripheral nerve repair using a poly (organo)phosphazene tubular prosthesis, Biomaterials 16 (1995) 347–353.
[30] Lemons M.L., Howland D.R., Anderson D.K., Chondroitin sulfate proteoglycan immunoreactivity increases following spinal cord injury and transplantation, Exp. Neurol. 160 (1999) 51–65.
[31] Lundborg G., Structure and function of the intraneuronal microvessels as related to trauma, edema formation, and nerve function, J. Bone Jt. Surg. Am. 57 (1975) 938–948.
[32] Lundborg G., Myers R., Powell H., Nerve compression injury and increased endoneurial fluid pressure: a "miniature" compartment syndrome, J. Neurol., Neurosurg. Psychiatry 46 (1983) 1119–1124.
[33] Mackinnon S.E., Pathophysiology of nerve compression, Hand Clin. 18 (2002) 231–241.
[34] Mackinnon S.E., Dellon A.L., Experimental study of chronic nerve compression, clinical implications, Hand Clin. 2 (1986) 639–650.
[35] Mackinnon S.E., Dellon A.L., Hudson A.R., Hunter D.A., Chronic nerve compression—an experimental model in the rat, Ann. Plast. Surg. 13 (1984) 112–120.
[36] Mackinnon S.E., Hudson A.R., Hunter D.A., Histologic assessment of nerve regeneration in the rat, Plast. Reconstr. Surg. 75 (1985) 384–388.
[37] Marotte L.R., An electron microscope study of chronic median nerve compression in the guinea pig, Acta Neuropathol. (Berl.) 27 (1974) 69–82.
[38] Martinez A.M., Canavarro S., Early myelin breakdown following sural nerve crush: a freeze-fracture study, Braz. J. Med. Biol. Res. 33 (2000) 1477–1482.
[39] Moon L.D., Asher R.A., Rhodes K.E., Fawcett J.W., Regeneration of CNS axons back to their target following treatment of adult rat brain with chondroitinase ABC, Nat. Neurosci. 4 (2001) 465–466.
[40] Morgenstern D.A., Asher R.A., Fawcett J.W., Chondroitin sulphate proteoglycans in the CNS injury response, Prog. Brain Res. 137 (2002) 313–332.
[41] Mosconi T., Kruger L., Fixed-diameter polyethylene cuffs applied to the rat sciatic nerve induce a painful neuropathy: ultrastructural morphometric analysis of axonal alterations, Pain 64 (1996) 37–57.
[42] Munger B.L., Bennett G.J., Kajander K.C., An experimental painful peripheral neuropathy due to nerve constriction. Axonal pathology in the sciatic nerve, Exp. Neurol. 118 (1992) 204–214.
[43] Neary D., Ochoa J., Gilliatt R.W., Sub-clinical entrapment neuropathy in man, J. Neurol. Sci. 24 (1975) 283–298.
[44] Nuytten D., Kupers R., Lammens M., Dom R., van Hees J., Gibels J., Further evidence for myelinated as well as unmyelinated fibre damage in a rat model of neuropathic pain, Exp. Brain Res. 91 (1992).
[45] O'Brien J., Mackinnon S., MacLean A., Hudson A., Dellon A., Hunter D., A model of chronic nerve compression in the rat, Ann. Plast. Surg. 19 (1987) 430–435.
[46] Ortman J.A., Sahenk Z., Mendell J.R., The experimental production of Renaut bodies, J. Neurol. Sci. 62 (1983) 233–241.
[47] Pindzola R.R., Doller C., Silver J., Putative inhibitory extracellular matrix molecules at the dorsal root entry zone of the spinal cord during development and after root and sciatic nerve lesions, Dev. Biol. 156 (1993) 34–48.
[48] Pires-Neto M.A., Braga-De-Souza S., Lent R., Molecular tunnels and boundaries for growing axons in the anterior commissure of hamster embryos, J. Comp. Neurol. 399 (1998) 176–188.
[49] Prinz R., Nakamura-Pereira M., De-Ary-Pires B., Fernandes D., Fabião-Gomes B., Bunn P., Martinez A., Pires-Neto M., Ary-Pires R., Experimental chronic entrapment of the sciatic nerve in adult hamsters: an ultrastructural and morphometric study, Braz. J. Med. Biol. Res. 36 (2003) 1241–1245.

[50] Renaut J., Système hyalin de soutènement des centres nerveux et de quelques organes de sens, Arch. Physiol. (Paris) 8 (1881) 846–859.
[51] Romero E., Cuisenaire O., Denef J.F., Delbeke J., Macq B., Veraart C., Automatic morphometry of nerve histological sections, J. Neurosci. Methods 97 (2000) 111–122.
[52] Rydevik B., McLean W.G., Sjostrand J., Blockage of axonal transport induced by acute graded compression of the rabbit vagus nerve, J. Neurol., Neurosurg. Psychiatry 43 (1980) 690–698.
[53] Sango K., Oohira A., Ajiki K., Tokashiki A., Horie M., Kawano H., Phosphacan and neurocan are repulsive substrata for adhesion and neurite extension of adult rat dorsal root ganglion neurons in vitro, Exp. Neurol. 182 (2003) 1–11.
[54] Silver J., Inhibitory molecules in development and regeneration, J. Neurol. 242 (1994) S22–S24.
[55] Skidmore R.A., Woosley J.T., Tomsick R.S., Renaut bodies. Benign disease process mimicking neurotropic tumor infiltration, Dermatol. Surg. 22 (1996) 969–971.
[56] Smith R.S., Koles Z.J., Myelinated nerve fibers: computed effect of myelin thickness on conduction velocity, Am. J. Physiol. 219 (1970) 1256–1258.
[57] Snow D., Watanabe M., Letourneau P.C., Silver J., A chondroitin sulfate proteoglycan may influence the direction of retinal ganglion cell outgrowth, Development 113 (1991) 1473–1485.
[58] Sobel R.A., Ahmed A.S., White matter extracellular matrix chondroitin sulfate/dermatan sulfate proteoglycans in multiple sclerosis, J. Neuropathol. Exp. Neurol. 60 (2001) 1198–1207.
[59] Sommer C., Galbraith J.A., Heckman H.M., Myers R.R., Pathology of experimental compression neuropathy producing hyperesthesia, J. Neuropathol. Exp. Neurol. 52 (1993) 223–233.
[60] Tanaka K., Zhang Q.L., Webster H.D., Myelinated fiber regeneration after sciatic nerve crush: morphometric observations in young adult and aging mice and the effects of macrophage suppression and conditioning lesions, Exp. Neurol. 118 (1992) 53–61.
[61] Thomas P.K., The connective tissue of peripheral nerve; an electron microscope study, J. Anat. 97 (1963) 35–42.
[62] Walz A., Anderson R.B., Irie A., Chien C.B., Holt C.E., Chondroitin sulfate disrupts axon pathfinding in the optic tract and alters growth cone dynamics, J. Neurobiol. 53 (2002) 330–342.
[63] Weis J., Alexianu M.E., Heide G., Schroder J.M., Renaut bodies contain elastic fiber components, J. Neuropathol. Exp. Neurol. 52 (1993) 444–451.
[64] Yick L.W., Wu W., So K.F., Yip H.K., Shum D.K., Chondroitinase ABC promotes axonal regeneration of Clarke's neurons after spinal cord injury, NeuroReport 11 (2000) 1063–1067.
[65] Yick L.W., Cheung P.T., So K.F., Wu W., Axonal regeneration of Clarke's neurons beyond the spinal cord injury scar after treatment with chondroitinase ABC, Exp. Neurol. 182 (2003) 160–168.
[66] Zuo J., Hernandez Y.J., Muir D., Chondroitin sulfate proteoglycan with neurite-inhibiting activity is up-regulated following peripheral nerve injury, J. Neurobiol. 34 (1998) 41–54.
[67] Zuo J., Neubauer D., Graham J., Krekoski C.A., Ferguson T.A., Muir D., Regeneration of axons after nerve transection repair is enhanced by degradation of chondroitin sulfate proteoglycan, Exp. Neurol. 176 (2002) 221–228.